



**The Contribution of Hydrogen Bonding to the
Photomechanical Response of Azobenzene-functionalized
Polyamides**

Journal:	<i>Journal of Materials Chemistry C</i>
Manuscript ID	TC-ART-01-2018-000319.R2
Article Type:	Paper
Date Submitted by the Author:	13-May-2018
Complete List of Authors:	Wie, Jeong Jae; Inha University, Polymer Science and Engineering; Air Force Research Laboratory Materials and Manufacturing Directorate; Azimuth Corporation Wang, David; Air Force Research Laboratory, Materials and Manufacturing Directorate; UES Inc Lee, Kyung Min; US Air Force Research Lab; Azimuth Corporation, White, Tim; Air Force Research Laboratory, Tan, Loon-Seng; US Air Force Research Lab, Materials & Manufacturing Directorate



ARTICLE

The Contribution of Hydrogen Bonding to the Photomechanical Response of Azobenzene-functionalized Polyamides

J. J. Wie,^{§,a,b,c} D. H. Wang,^{§,a,d} K. M. Lee,^{a,b} T. J. White^{a,*} and L.-S. Tan^{a,*}

Received 00th January 20xx,
Accepted 00th January 20xx

DOI: 10.1039/x0xx00000x

www.rsc.org/

Photomechanical effects in materials can directly convert light stimulus into mechanical work. The magnitude of the photogenerated work is directly associated with the material stiffness (modulus). Here, we report the synthesis of an azobenzene-functionalized polyamide (azoPA) and demonstrate its room-temperature photomechanical response. The comparatively large photomechanical response of this high stiffness material is enabled by light-induced, azobenzene-assisted dissociation of inter-chain hydrogen bonding within the polymer backbone. The photomechanical response of the azoPA is directly contrasted with an analogous azobenzene-functionalized polyimide (azoPI) to illustrate the influence of intermolecular interactions.

Introduction

Photomechanical effects in macromolecules have been investigated for nearly 50 years.¹ In that time, considerable research has focused on the synthesis of new materials and the characterization of the photo-induced effects. Recently, these materials have been subject to intense investigation, largely motivated by the prospect of employing photomechanical effects to realize shape reconfigurable devices,²⁻³ energy harvesting,⁴⁻⁵ and soft robotics.⁶⁻⁸

Among the photo-switchable chromophores,⁹ azobenzene is arguably the most-utilized photochromic unit in the development of photoresponsive amorphous, crystalline, and liquid crystalline polymers because of its excellent thermal stability, resolved isomeric forms, unique optical nonlinearities,¹⁰ and ability to form birefringent gratings/surface-relief structures when subjected to conventional or polarization holography.^{11,12} The photoinduced responses of these polymeric materials are triggered by most commonly trans-cis isomerization upon irradiation of 365 nm UV light. The trans-cis isomerization reduces the molecular axis of azobenzene from 9 Å (trans) to 5.5 Å (cis).¹³

Photomechanical effects are commonly visualized in a cantilever geometry, in which the length is larger than the width, and considerably larger than the thickness. Upon exposure, light triggers a deflection (bending) of the cantilever. The mechanics of the deformation are analogous to a bimetallic

strip. Due to the typically large concentration of absorbing material as well as the thickness, the light is attenuated throughout the material thickness. This results in a gradient in strain that mirrors the light intensity profile. In the case of UV light exposure, continuous irradiation eventually photobleaches the material to the cis isomer form.

On the other hand, distinctive mechanical outcomes can be observed by irradiation with blue-green light, near the isosbestic absorption of the isomeric forms of azobenzene.^{12,15} When linearly polarized blue-green light is incident on azobenzene-functionalized polymeric materials, a small but measurable fraction of azobenzene can reorient orthogonally to the orientation of the electric field vector of the polarized light source, attributable to both the rotational freedom of the N-N bond (in photoexcited azo with broken π -bond) and the dichroic absorbance of both the trans and cis isomeric forms.¹⁶ The local reorientation of azobenzene results in a highly stable, optically fixed shape in polymeric glasses, without a substantial concentration of the thermally sensitive cis isomer.¹⁷⁻²⁵ Further, the directionality of the strain can be dictated by the orientation of the linearly polarized light to the principal axes of the material (in a cantilever geometry). This allows for both contractile or expansive control of the bending direction, namely, towards or away from the light source, respectively.¹⁴

While much of the recent literature has focused on the preparation and characterization of azobenzene-functionalized liquid crystalline polymer networks (azo-LCNs),²⁶⁻²⁹ comparatively less attention has been paid to the high performance polymeric materials that may have some advantages, particularly in applications in load-bearing or extreme environments.³⁰⁻³² For example, polyimides and polyamides are known to maintain exceptional mechanical, thermal, and chemical resistant properties as well as excellent dimensional stability and abrasion resistance that are suitable for applications such as engineering plastics, fibers, wire coatings, machine parts, etc. Prior research examining the

^a Materials & Manufacturing Directorate, Air Force Research Laboratory, Wright-Patterson Air Force Base, Ohio 45433-7750, USA. Email (Loon-Seng Tan): loon.tan@us.af.mil; Email (Timothy J. White): timothy.j.white.24@us.af.mil.

^b Azimuth Corp. Dayton, OH 45432, USA

^c Department of Polymer Science and Engineering, Inha University, Incheon 22212, South Korea

^d UES Inc., Dayton Ohio, 45432, USA

† Electronic Supplementary Information (ESI) available: [POM, DMA and FTIR results of azoPA and azoPI]. See DOI: 10.1039/x0xx00000x

§ These authors contributed equally

photoinduced deformation of high performance polymers has been mostly limited to polyimides. The photomechanical response of azobenzene-functionalized polyamides (azoPA) are still largely unexplored.

These two classes of high performance polymers are structurally differentiated by the prevalence of hydrogen bonds in polyamides. The strong influence of hydrogen bonding (H-bonding) in the structure-property-performance of synthetic polyamides and natural polypeptides has been well-documented.³³⁻³⁴ The strengths of various H-bonding modes determine the structural and mechanical integrity of proteins, DNA, and supramolecular polymers in conjunction with other intermolecular forces (van der Waals, electrostatic, hydrophobic, and steric forces).³⁴⁻³⁵ While proper manipulation of H-bonding interactions is an important design tool for advanced functional polymeric materials,³⁶⁻⁴⁰ particularly in enhancing (static) mechanical properties such as modulus and compressive strength,⁴¹⁻⁴² it is also important to be cognizant of the opposing influence that H-bonding may encumber on certain primary effects in the dynamic properties of functional materials. For example, inter-chain H-bonding have been implicated in suppressing the photoinduced birefringence of azobenzene-functionalized poly(amide-imide)s.⁴³

This study assesses the performance of polyamides in finding end use as photomechanical actuators. Towards this end, it is necessary to determine how hydrogen bonding contributes to both the photochemical and photomechanical responses. To frame this study, we correlate the response of the polyamide reported here to the photomechanical output of a structurally similar azobenzene-functionalized polyimide. Similar to previous studies, we have characterized the photomechanical responses of these materials by monitoring the deflection (visualization of strain) of cantilevers^{17-18,44} and measuring photogenerated stress^{18,45-46} in tension. The azoPA examined here exhibits large photo-directed deflection upon exposure to linearly polarized blue (445nm) light. The influence of light irradiation on inter-chain H-bonding will be discussed.

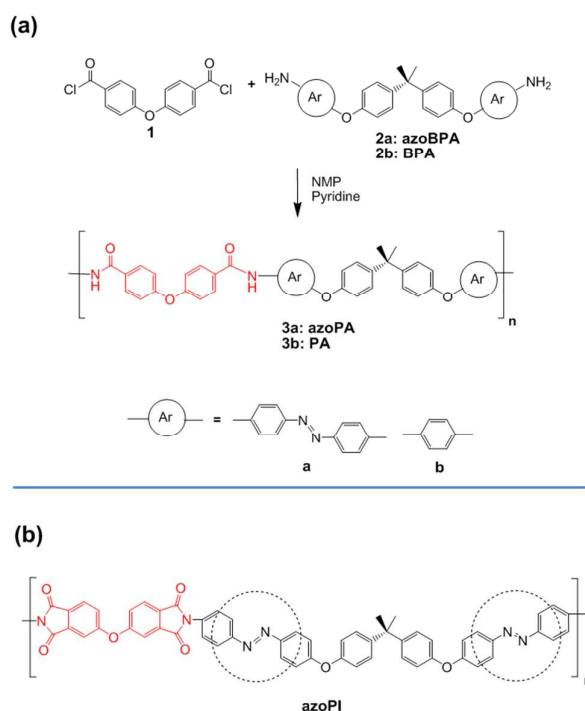
Results and Discussion

A number of parameters can influence the photomechanical responses of azobenzene-functionalized polymeric materials including azobenzene concentration^{47,48}, chemical composition^{18,46,48}, crystallinity¹⁸, molecular alignment⁴⁹, modulus⁴⁶, free volume,⁴⁴ and segmental mobility.⁴⁷ The largest photomechanical responses reported to date in high-performance azobenzene-functionalized polyimides (azoPI's) have been observed in materials in the amorphous state that maintain sub- T_g transitions (segmental or β -relaxation). Here, our focus is to investigate whether the intermolecular (*inter-chain*) hydrogen-bonding that is characteristic of polyamides (PA's) and responsible for their high T_g and modulus would affect the photomechanical response. To isolate this contribution, we have intentionally synthesized an amorphous azobenzene-functionalized polyamide (azoPA) that *does not* exhibit a sub- T_g transition (*vide infra*). To our knowledge, this

is the first examination of photoinduced responses in an azoPA film subject to hydrogen bonding.⁵⁰

Material Synthesis.

The chemical structures of azoPA, azoPI, and a control polyamide without azobenzene (PA) employed in this study are shown in **Scheme 1**. The extended structures of azoPA and azoPI are quite similar except for the additional $-C(=O)-$ moieties in azoPI. As both azoPA and azoPI have two azobenzene moieties per repeat unit, and qualitatively comparable molecular length for their repeat units, it can be reasonably assumed that they have effectively ($\pm 6\%$)⁵¹ the same molar azobenzene chromophore concentration. The polyamides, azoPA and PA were prepared from 4,4'-oxydibenzoyl chloride (**1**) and the respective diamine monomers, 2,2-bis{4-[4-(4-aminophenyldiazenyl)phenoxy]phenyl}propane (**2**) and 2,2-bis[4-(4-aminophenoxy)phenyl]propane (**3**) in N-methylpyrrolidone (NMP) and using pyridine as the HCl scavenger. The polyimide counterpart, azoPI, was prepared similarly as previously reported.⁴⁷



Scheme 1: (a) Synthesis of the azobenzene-functionalized polyamide (**3a**, azoPA) and structurally similar polyamide without azobenzene moiety (**3b**, PA). (b) Repeat-unit structure of the structurally similar azobenzene-functionalized polyimide (azoPI).

Both azoPA and azoPI are glassy (amorphous) materials as evidenced by their broad and featureless wide-angle x-ray diffraction (WXAD) profiles of their films (**Fig. 1**) and their polarized optical micrographs confirm their isotropic nature

when examined between cross-polarizers at the angles of 0° , 90° , and 180° (Fig.S1, Supporting Information).

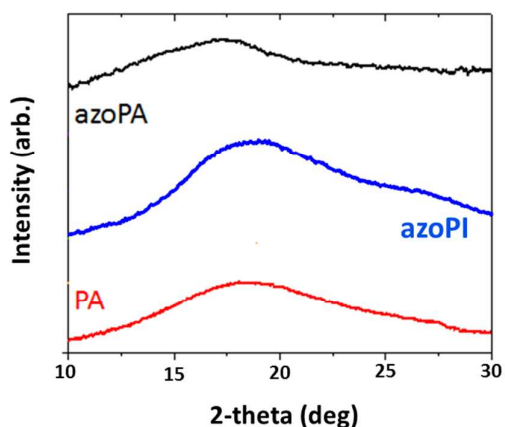


Fig. 1. WAXD profiles for azoPA and PA as well as azoPI indicate that they are all amorphous materials.

Thermal Characterization.

The thermal properties of the new polymers, namely azoPA and PA were first evaluated by differential scanning calorimetry (DSC) and thermogravimetric analysis (TGA), both using the same scanning rate of $10^\circ\text{C}/\text{min}$.

As summarized in Table 1, the glass transition (T_g) detected for azoPA by DSC at 220°C is $\sim 17^\circ\text{C}$ higher than the T_g of PA because of the higher polymer backbone rigidity endowed by trans-azobenzene moieties in azoPA. The difference in the T_g values is confirmed by the measurements by dynamic (thermo)mechanical analyzer (DMA). The T_g of azoPI, while not detected by DSC under the same scanning conditions, is determined by DMA to be at $\sim 230^\circ\text{C}$.

Table 1. Summary of thermal analysis results for polymers measured in air and nitrogen atmosphere.

Sample	T_g^a , [DMA] ^b ($^\circ\text{C}$)	$T_{d5\%}^c$ ($^\circ\text{C}$) in air	$T_{d5\%}^c$ ($^\circ\text{C}$) in N_2
azoPA, 3a	220 ^a [227] ^b	421	386
azoPI	ND ^a [230] ^b	451	420
PA, 3b	203 ^a [210] ^b	421	431

Note: (a). DSC scanning rate of $10^\circ\text{C}/\text{min}$ under N_2 ; ND=Not Detected by DSC. (b). T_g measured from the peak of $\tan \delta$ (DMA) as an average value taken from four measurements. (c). Temperature at which 5% weight loss recorded on TGA thermogram obtained with a heating rate of $10^\circ\text{C}/\text{min}$.

The TGA results (Table 1) indicate that all the materials tested here display relatively high thermal stability, characterized by the temperatures for 5wt% weight loss ranging between $421\text{--}451^\circ\text{C}$ in air (azoPI>azoPA~PA), and $386\text{--}431^\circ\text{C}$ in nitrogen (PA>azoPI>azoPA).

In addition, the comparative results for azoPA and azoPI indicate that the thermooxidative degradation process is more

gradual and more complex for azoPA than azoPI (Fig.2a). Even though azoPA starts to degrade at temperatures lower than for azoPI, it becomes slightly more resistant to oxidative degradation than azoPI in the carbonization region of $\sim 550\text{--}700^\circ\text{C}$.

Notably similar to our previous observations,^{46,52} the $T_{d5\%}$ values of these materials in air are found to be $\sim 31\text{--}35^\circ\text{C}$ (Table 1) higher than measurements in a nitrogen atmosphere (Fig.2b). In general, polymers are more stable (higher degradation temperatures) in nitrogen than in air. These unusual observations are explained by the oxidation of the azo ($\text{N}=\text{N}$) bonds, possibly via the formation of azoxy ($-\text{N}=\text{N}(\text{O})-$), azodioxy ($-(\text{O})\text{N}=\text{N}(\text{O})-$), and/or nitro ($-\text{NO}_2$), resulting in weight gain in air, and offsetting the weight loss due to the usual thermo-oxidative degradation processes that occurred concurrently. With the repeated observations, such unusual thermal (TGA) behavior appears to be rather characteristic of azobenzene-functionalized, high-performance polymers.

However, the azobenzene moiety is apparently the thermally weak link in azoPA when the thermal stability of azoPA and PA is compared. This is likely due to the thermodynamically favored formation of N_2 from azoPA during thermal degradation process, resulting in the observed trend PA>azoPI>azoPA (Table 1).

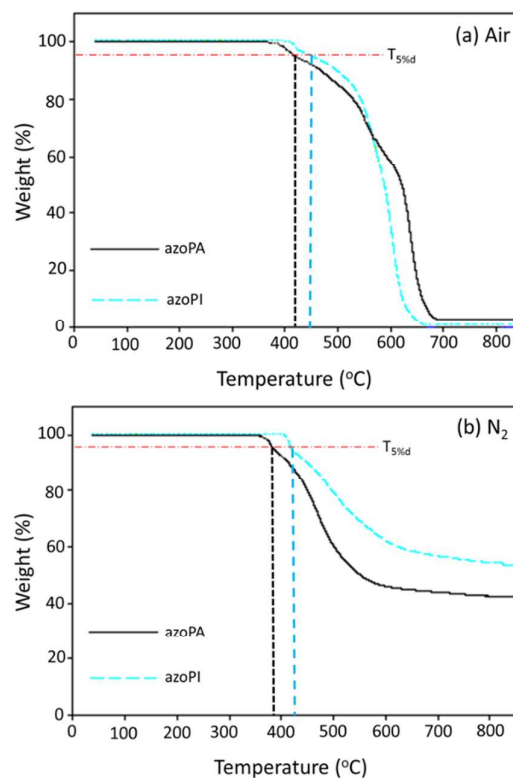
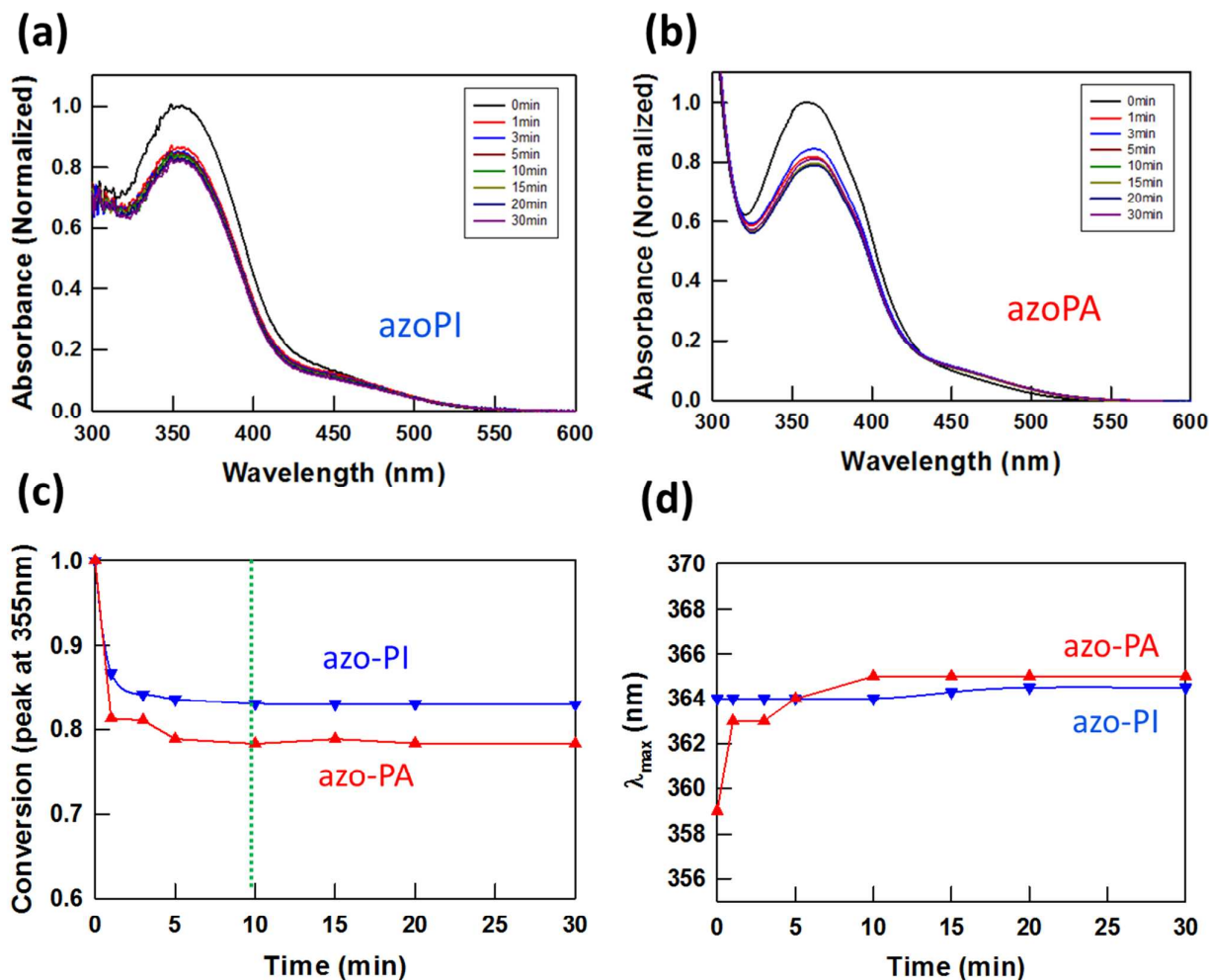


Fig. 2. Plots of thermogravimetric analysis for azoPA and azoPI in (a) air and (b) nitrogen atmospheres. The presence of azobenzene in both cases reverses the typical observed trend on the thermal vs. thermooxidative stabilities for aromatic polymers.

UV-Vis Characterization.

Fig. 3 (a) Normalized absorption spectra of azoPI taken at a series of time exposure to 50 mWcm^{-2} , 445 nm irradiation. (b) Absorption spectra of azoPA upon



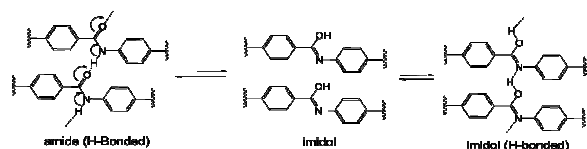
exposure to 50 mWcm^{-2} 445 nm irradiation. (c) Conversion of trans-isomer to cis-isomer by as a function of irradiation time for azoPA and azoPI. The absorbance at 355 nm before irradiation is taken as 100% (1.0) trans-isomer. Green dotted line marks approximately the onset of photostationary state. The trans-cis photoconversion (%) was determined by the following equation: $[(A_0 - A_t)/A_0] \times 100\%$ where A_0 and A_t are normalized absorbance values at $\lambda_{\text{max}}=355\text{nm}$ before and 30 min after blue-light irradiation, respectively. (d) Wavelength at peak absorbance during irradiation for azoPA and azoPI.

To provide a baseline to enable the comparison of the photomechanical responses of the azoPA and azoPI, we have first measured the solid-state UV-Vis spectra of their spin-cast films to confirm that they indeed exhibit negligible differences in their characteristics in absorption and photoconversion. This is evident in the UV-Vis absorption spectra of azoPI (**Figure 3a**) and azoPA (**Figure 3b**) taken intermittently before and during photomechanical experiment with a linearly polarized, i.e. with the electric field vector in parallel to the long axis of the cantilever ($E//x$), 445nm (blue) LED light. Before irradiation, the UV-vis absorption spectra establish the baseline for the trans configuration of the azobenzene chromophores within both polymers that is assumed to be 100% under ambient conditions. Irradiation with the blue LED light at an intensity of 50 mWcm^{-2} induces both trans-cis isomerization and cis-trans reorientation

processes of azobenzene. This is evident in both samples showing a slight decrease in absorbance at 365 nm ($n \rightarrow \pi^*$ transition) as well as a slight increase in absorption at 450 nm (attributed to the formation of cis-isomers). Following the decay of λ_{max} at 355nm, **Figure 3c** depicts that the onset of the photostationary state for both polymers is reached after 10 min of the blue light irradiation. At this stage, the trans-cis conversion for azoPI (~83%) is found to be somewhat higher than that of azoPA (~78%). Thus, it is estimated that a 50 mW/cm^2 , blue light can induce ~17-22% yield of cis-isomers in azoPI and azoPA. As the same linearly polarized, blue light has previously been shown to induce comparable azobenzene isomerization/reorientation in azoPI, contributing to the mechanical response,⁴⁶ **Figure 3a-c** suggests that the

photosensitivity and mechanical output of the azoPA and azoPI would be quite similar after having reached photostationary state.

In addition, the influence of light on H-bonding in the presence of azo-chromophore is hinted by following the subtle change in the λ_{\max} of the irradiated azoPA and azoPI films with time (**Figure 3d**). Before irradiation, the λ_{\max} of azoPA is 359 nm. During the course of 30-minute exposure to the same blue light, the λ_{\max} (azoPA) progressively moves to longer wavelengths, and after 15 minutes of light exposure, it remains at 365nm despite further irradiation for another 15 minutes. Under the same conditions, λ_{\max} of azoPI exhibits a negligible shift (0.5 nm). It is speculated that the red-shift



Scheme 2: Proposed photo-induced amide-imidol tautomerization for azoPA with the benzanilide moiety in trans conformation. Dimeric cis-conformer of benzanilide molecules in frozen methylcyclohexane matrix was proposed in reference 53a. In solid state, it is likely that the breaking of H-bonding (proton-transfer) in amide and formation of imidol are proceeding in concert.

in azoPA during irradiation is stemming from the occurrence of a photoinduced proton-transfer amide-imidol tautomerization that has been attributed to the origin of the dual fluorescence observed for benzanilide in a frozen hydrocarbon matrix.⁵³ A modified amide-imidol tautomerization process for benzanilide in azoPA is proposed in Scheme 2.

The red-shift in azoPA may be explained by the presence of imidol, *viz.* the more conjugated isomer of amide, upon photo-excitation. In addition, both amide and imidol (a.k.a. imide acid) in trans conformation can engage in interchain hydrogen bonding but the angular mode of H-bonding (i.e. in imidol) is known to be weaker than the linear mode (i.e. in amide).⁵⁴

Therefore, we speculate that such photoinduced tautomerization⁵³ in azoPA to be a minor process, but not insignificant; and also likely to be strongly coupled with the azobenzene photoisomerization processes leading to the rupture of H-bonding. The dissociation of H-bonds, and the possible occurrence of amide-imidol tautomerization are further supported by the comparative FT-IR examination of PA (with no azobenzene moieties), which shows practically no change in the distribution of free N-H and H-bonded N-H vibrations before and after the same irradiation conditions (*vide infra*).

Photomechanical & Dynamic Mechanical Characterization.

The influence of light irradiation on the mechanical properties of azoPA and azoPI were investigated by an in-situ (i.e. real-time off-on-off) irradiation with the blue LED light and at the same intensity of 50 mWcm⁻² as that for the UV-Vis experiment) during the dynamic mechanical analysis (DMA) experiments, using the experimental set-up as reported previously (ambient temperature & in-situ irradiation).⁴⁵ Before the exposure to light, the elastic storage modulus (E') at 25 °C were found to be ca. 2.5 GPa and ca. 2.0 GPa for azoPA and azoPI, respectively. About 60 seconds after light-on, the modulus (E') of both azoPA and azoPI would decrease to ~1.8 GPa (ca. 28% & 10% drop for azoPA and azoPI, respectively), and would remain practically unchanged thereafter (**Figure 4a**). Given the assumption that under the same irradiation conditions, the moduli of azoPA and azoPI are virtually the same, it is reasonable to deduce that both polymer backbones are structurally quite similar, and it follows that only at sufficiently high degree if not complete, the rupture of interchain H-bonding in azoPA must have occurred under these circumstances. In addition, it is known that irradiation of photoresponsive materials to light that induces trans-cis photoisomerization or trans-cis-trans reorientation can result in photo-softening.^{55,56} In our case, while the magnitude of photo-softening is found to be much larger in azoPA than azoPI, both decreases are not on the scale of photofluidization that requires several decades in the drastic drop of modulus.^{57,58}

As the photomechanical response of azoPI is known to be enhanced by the molecular motion below its T_g ,⁴⁷ we would need to clarify whether the photosoftering of azoPA has originated solely from the photoinduced disruption of intermolecular H-bonds and/or partially from enhanced intramolecular sub- T_g relaxation. Thus, temperature-resolved DMA experiments for both the azoPA and azoPI cantilevers were carried out before and after 10 min of 445 nm light irradiation at the same intensity (50 mWcm^{-2}).

The photomechanical response of azoPI as measured by DMA is shown in **Figure 4b**. As discussed in our previous report,⁴⁷ light irradiation provides an enhanced intramolecular segmental mobility to azoPI, which is responsible for the large photomechanical deformation observed. Here, after 10 minutes of 445 nm light irradiation, the enhanced E'' is observed for

azoPI over the entire temperature ranges for the sub- T_g transition, designated as β -transition (ca. 27°C - 167°C). The molecular motion related to this β -transition is attributed to the para-phenylene ($-\text{C}_6\text{H}_4-$) ring rotation.⁵⁹ It is noteworthy that the peak position of E'' remained effectively constant even after the light irradiation. As a consequence from the enhanced β -relaxation process, light irradiation apparently reduced the T_g azoPI by 5°C (from 230°C to 225°C).

Figure 4c depicts the photomechanical response of azoPA measured by DMA before and after the light irradiation. Regardless of the light irradiation, the modulus loss (E'') of azoPA has remained constant. However, a pronounced shift in the α -transition (i.e. T_g drops from 226°C to 210°C) is apparent upon exposure to 445nm light for 10 min. The photoinduced decrease in E' as well as the accompanying shift in T_g could be attributed to the dissociation of intermolecular H-bonding in azoPA. Practically, the absence of any sub- T_g transition in azoPA in the range of 27°C - 167°C precludes the possibility of its involvement in the photo-softening.

These results support the tentative conclusion that under irradiation conducive to photomechanical responses for both azoPA and azoPI, only the interchain H-bonding and no sub- T_g effect are involved in azoPA, and vice versa for azoPI. The exclusive involvement of H-bonding in the photomechanical effect of azoPA is further examined by Fourier-transform infrared (FT-IR) spectroscopy.

FT-IR Characterization.

FT-IR technique is very useful to identify the nature of H-bonding in amides as well as probing the bonding changes with an input of excitation energy (thermal or photo).

The FT-IR spectra for the thin films ($\sim 20 \mu\text{m}$) of azoPA and the analogous polyamide without the azobenzene functionality (PA) that were taken before and immediately after exposure to 445nm blue laser light (120 mW/cm^2) for 1 hour are superimposed in **Figure 5a**. In the finger-print region of both spectra (**Fig.5b**), the characteristic amide I (carbonyl stretch) and

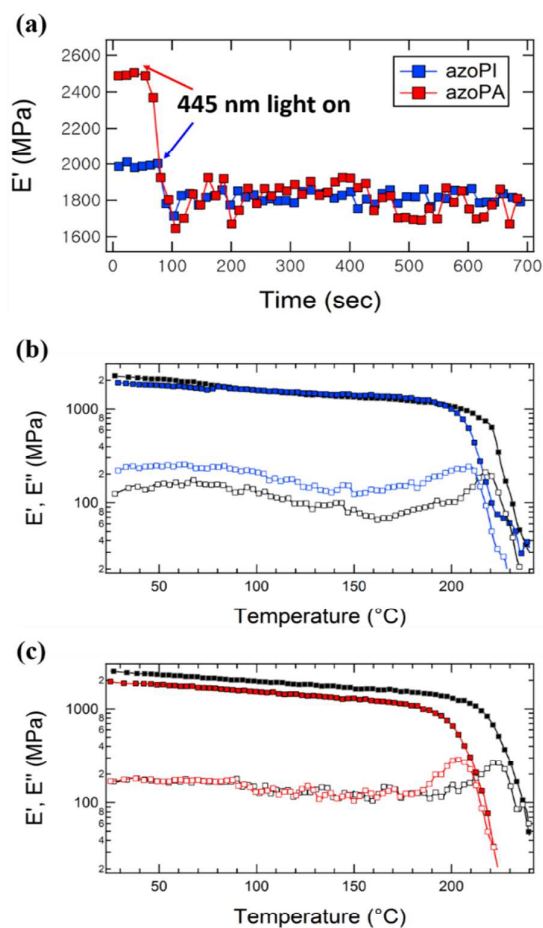


Fig. 4 (a) Change in storage modulus during continuous irradiation for azoPA (■) and azoPI (■) as measured by DMA; (b) Temperature-resolved storage (E' , filled square symbol) and loss moduli (E'' , unfilled square symbol) of azoPI before (black) and after (red) light irradiation. (c) Temperature-resolved storage (E' , filled square symbol) and loss moduli (E'' , unfilled square symbol) of azoPA before (black) and after blue-light irradiation) measured by DMA.

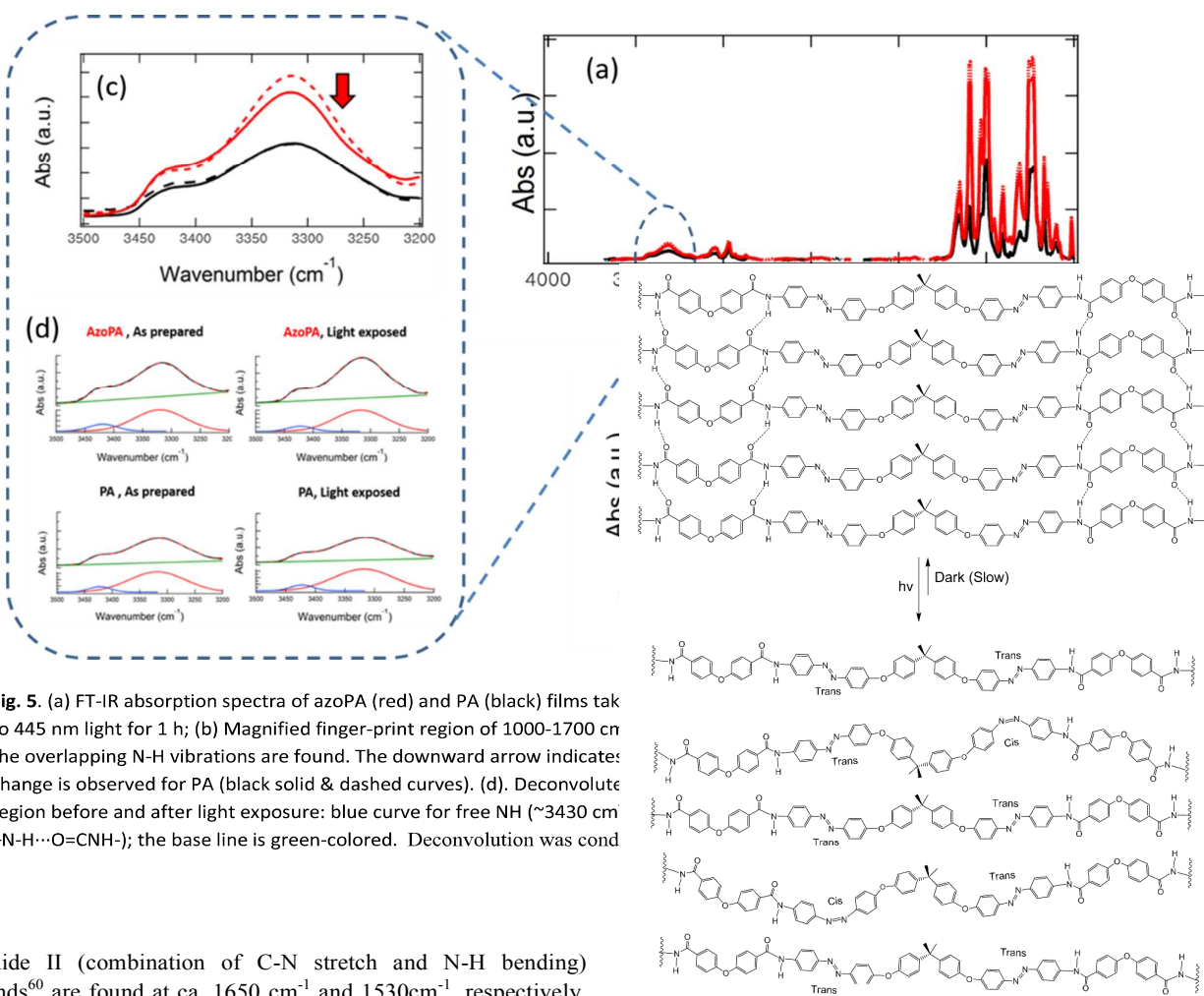


Fig. 5. (a) FT-IR absorption spectra of azoPA (red) and PA (black) films taken at 445 nm light for 1 h; (b) Magnified finger-print region of 1000-1700 cm^{-1} where the overlapping N-H vibrations are found. The downward arrow indicates the change observed for PA (black solid & dashed curves). (d). Deconvoluted region before and after light exposure: blue curve for free NH (~3430 cm^{-1} -N-H...O=CNH-); the baseline is green-colored. Deconvolution was conducted

amide II (combination of C-N stretch and N-H bending) bands⁶⁰ are found at ca. 1650 cm^{-1} and 1530 cm^{-1} , respectively. Because of the local symmetry of the azobenzene moiety in azoPA and by comparison with FTIR of PA (Fig. S3), no azo (N=N) vibration for azoPA can be assigned in the range of 1400-1450 cm^{-1} expected for the unsymmetrical azobenzene compounds.⁶¹ In addition, the spectra taken after light irradiation show an obvious shift in absorbance for azoPA, but practically no change in that regard for PA. As expected, no new vibration bands due to chemical changes appear in this region for both azoPA and PA after irradiation.

The IR vibrations associated with intermolecular H-bonding in polyamides are typically detected in the wavenumber ranges between 3225 and 3280 cm^{-1} for the H-bonded N-H band,⁶² and the free N-H band for polyamides is observed at around 3448 cm^{-1} .^{63,64} As for the strong propensity of amides to associate,

Scheme 3: Idealized presentation of H-bonding network structure of azoPA, which under linearly polarized blue light irradiation, transforms into an excited state structure driven and coordinated by the processes of azobenzene trans-to-cis photoisomerization, dissociation of inter-chain H-bonds, and trans-cis-trans reorientation processes, reaching a photostationary state. The thermal reformation of inter-chain H-bonding in darkness, presumably in tandem to the cis-trans isomerization of azobenzene, is slow and likely to be incomplete. For clarity, (i) while the weaker H-bonding between N-H and ether-O (not shown) is also possible, only interchain H-bonding between N-H and carbonyl-O is shown; and (ii) imidol moiety, which may be part of the excited state structure for azoPA, is not shown here.

Schroeder and Cooper reported that nearly all of the N-H groups are H-bonded at room temperature for both crystalline and amorphous nylon films based on the FT-IR spectra of the free and H-bonded N-H stretching regions (3440 and 3300 cm^{-1} , respectively).⁶⁵

The photoinduced dynamics of inter-chain H-bonding was elucidated for azoPA by contrasting to PA on their spectral changes in the wavenumber ranges of 3200 - 3500 cm^{-1} , which is magnified in **Figure 5c**. In this region, both azoPA and PA exhibit two overlapped peaks. Deconvolution of the FTIR spectra of azoPA and PA (**Figure 5d**) have revealed a small peak at 3430 cm^{-1} and a large peak at 3325 cm^{-1} , which are assigned to the vibrations of free N-H and H-bonded N-H (amide) bonds, respectively. The values of computed peak area of deconvoluted FTIR spectra for azoPA and PA are summarized in **Table 2**.

It should be pointed out that H-bonded NH..O population proportional to the peak area includes not only NH..O(carbonyl) bonds but also NH..O(ether) population. Before exposure to light, the calculated absorption peak area (APA, in arbitrary unit or a.u.) directly related to the population of the free N-H bonds (3430 cm^{-1}) of azoPA is 3.16 a.u. , which is higher than the APA for PA (1.7 a.u.), and the APA for the population of H-bonded N-H is 25.16 a.u. which is also higher than that of PA (16.84 of free N-H population is increased by 0.85 a.u. (or 26.9%) and that of H-Bonded N-H is decreased by 2.66 a.u. (or -10.6%) for azoPA, while PA shows little or no change over the course of 1-hour exposure, assuming the computation error of $\pm 0.6\text{ a.u.}$ The relatively large increase (~ 26 - 27%) in the population of free N-H bonds, i.e. the decrease in inter-chain H-bonding, would promote longer-range mobility of polymer chains during the trans-cis-trans reorientation process, resulting in the strain generation. In conjunction with the results from the UV-vis and real-time photomechanical experiments, we postulate that (a) under continuous light irradiation, as the dissociation of interchain H-

Table 2. Deconvoluted peak values in arbitrary unit (a.u.) of FT-IR spectra of azoPA and PA before and after irradiation with polarized 445 nm light.^a

Sample	[Free N-H] (a.u.)	Change in [Free N-H] after irradiation	[H-Bonded N-H] (a.u.)	Change in [H-Bonded N-H] after irradiation
AzoPA, Before irradiation	3.16	26.9%	25.16	-10.6%
AzoPA, After irradiation	4.01	($\pm 0.6\%$)	22.50	($\pm 0.6\%$)
PA, Before irradiation	1.74	0%	16.84	0%
PA, After irradiation	1.75	($\pm 0.6\%$)	16.73	($\pm 0.6\%$)

a. 0% - 0.6% change in PA was computed for both the free N-H (increase) and H-bonded N-H (decrease) populations. Since there is no change in the UV-vis and DMA results before and after blue-light irradiation, indicating that no H-bonding in PA (i.e. without any azobenzene) is being broken during irradiation, the overall error of computation is therefore assumed to be $\pm 0.6\%$.

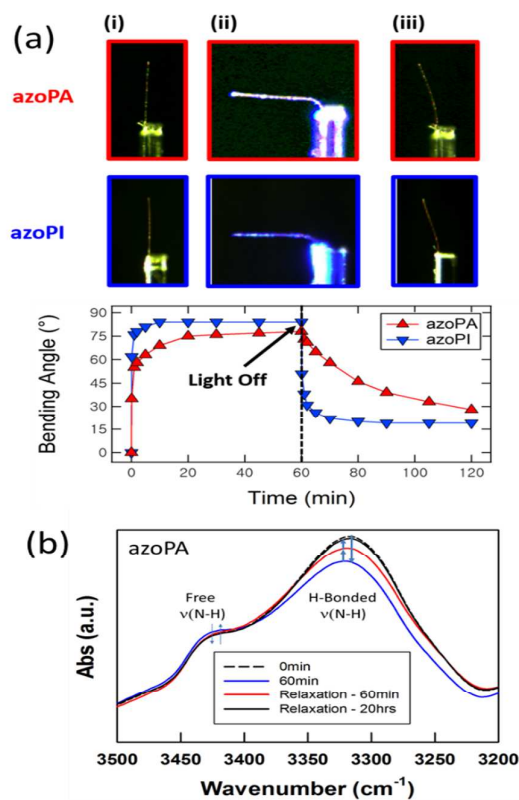


Fig. 6 (a) Time-resolved measurement of photomechanical responses of azoPA (\blacktriangle) and azoPI (\blacktriangledown) upon irradiation of 120 mW/cm^2 cw blue laser light for 60 min followed by allowing them to relax in dark for 60 min. The photos (i), (ii), and (iii) were taken at time = 0, 60 and 120 min, in that order. (b) The breaking and reformation of interchain H-bonding in azoPA is visualized by the decay of H-bonded $\nu(\text{N-H})$ and growth of free $\nu(\text{N-H})$ over 60 min of blue light irradiation (down & up arrows).

bonds in azoPA in sufficiently large number, if not all, occurs, azoPA material would assume a backbone configuration akin to that of the azoPI; (b) the initiation and propagation of the azobenzene photoisomerization and reorientation processes are the pre-requisite conditions. Based on these postulates, we propose a mechanism to explain the photomechanical behavior of azoPA (as an example for the azobenzene-functionalized system with H-bonding) that is depicted in Scheme 3 and described in the caption.

Photomechanical Effect & H-Bonding Reformation

As it is becoming clear from the foregoing discussion, the indirect influence of light on the rupture of intermolecular H-bonding and the concurrent reduction in stiffness are responsible in an enhanced photomechanical response of azoPA. To complete this study, we have examined the photomechanical behavior cycle (120 min) of both the azobenzene-functionalized polymers.

Fig. 6 depicts the temporal evolution of the photoinduced deflection of the azoPA and AzoPI cantilevers over the course

of one-hour irradiation with the blue laser light at 120 mWcm^{-2} , followed by relaxation with light-off for another hour. Both materials reach the photo-stationary state and depict their maximal deflections (78° and 85° bending angles for azoPA and azoPI, respectively) within an hour. The relaxation in dark of the photoinduced deflection of the cantilever (visualization of photoinduced strain) was then monitored over the course of 1 hour. As apparent from the plot in Fig. 6a, both photomechanical deformation and the relaxation in dark are slower for azoPA than for azoPI, probably because of the reformation of the H-bonds in azoPA. Based on the assumption that the degree of photo-induced bending is proportional to the amount of cis-azobenzene isomers generated, a rough estimate from the plot of bending angle vs time (Fig. 6a) gives the value of half-life ($\tau_{1/2, \text{Cis}}$) for the cis-isomers generated at photostationary state in azoPI to be ~ 43 sec. as determined at when bending angle is relaxed to $\sim 42\text{--}43^\circ$, and $\tau_{1/2, \text{Cis}}$ for azoPA similarly determined to be ~ 30 min at bending angle = 39° .

The relatively slow reformation of H-bonds in azoPA in the absence of light after having been irradiated with the blue laser light for 60 min is supported by the recovery of its FT-IR spectrum, especially the wavelength region ($3200\text{--}3500 \text{ cm}^{-1}$) where the N-H vibrations are found (Fig. 6b). In addition, the original DMA profile for azoPA that has been subjected to the same blue light irradiation and subsequent storage in darkness for 2 days is also completely restored, i.e. storage modulus to ~ 2.5 GPa and T_g to $\sim 227^\circ\text{C}$ (Fig. S2).

On a further note, it is apparent that under appropriate photo-excitation conditions, the strength of H-bonded network in azoPA is not strong enough to impede the photomechanical response driven by azobenzene chromophores, whose photoisomerization process can generate strain more than sufficient to overcome such molecular hindrance. However, H-bonded network in azoPA provides higher ground state stiffness than azoPI, and in turn, higher dimensional stability during operational stand-down.

Conclusions

A newly synthesized, high T_g , and high modulus azobenzene-functionalized polyamide (azoPA) has shown promise as a photomechanical material. Here, we illustrate that the large photomechanical response of the azoPA is possible upon the dissociation of *inter-chain* hydrogen bonding. This is in part confirmed by the observation of the dynamic rupture of H-bonds revealed and quantified by FTIR examination of the free and H-bonded N-H peaks. The overall light-to-work process is driven by the azobenzene photoisomerization processes, which possibly coupled with a photoinduced proton-transfer amide-imidol tautomerization. Based on the results from the time-resolved monitoring of photoinduced deflection and dark relaxation (via observation by FTIR and DMA), the glassy azoPA appears to have similar photo-response, but it is also slower to recover than an analogous azobenzene-functionalized polyimide (azoPI) with unencumbered, sub- T_g segmental mobility. While the reformation of interchain H-bonding in

azoPA may be responsible for slowing down the recovery, it definitively contributes to the full recovery of the thermomechanical properties after relaxation in dark. This comparative study suggests that both intra- and inter-chain modes of mobility may be utilized in macromolecular design strategies to manipulate or modulate activation/relaxation p to improve the performance of these materials to allow them to realize practical implementations.

Experimental

Materials.

The diamine monomers, 2,2-bis[4-(4-aminophenoxy)phenyl]propane (BPA) was purchased TCI America, and 2,2-bis[4-(4-aminophenyldiazenyl)phenoxy]phenyl]-propane (azoBPA) was synthesized according to previously reported procedure.⁴⁶ All other reagents and solvents were purchased from Aldrich Chemical Inc. and used as received, unless otherwise noted.

4,4'-Oxydibenzoyl chloride (1, ODBC). Into a 250 mL three-necked flask equipped with a magnetic stir bar, a condenser and nitrogen inlet and outlet were placed 3,3'-oxybis(benzoic acid) (1; 15.0 g, 58.1 mmol), thionyl chloride (75 mL) and dimethylformamide (several drops). The mixture was refluxing with agitation until the solid disappeared. Excess thionyl chloride was evaporated. The residual solid was recrystallized from hexanes to yield 13.0 g (75.8%) of white crystals; m.p. $89.6\text{--}91.2^\circ\text{C}$. $^1\text{H-NMR}$ ($\text{CDCl}_3/\text{DMSO-d}_6$, δ in ppm): 6.52–6.54 (d, 4H, Ar-H), 7.49–7.51 (d, 4H, Ar-H). ATR-IR (cm^{-1}): 3099, 3075, 2808, 2541, 1758, 1731, 1678, 1578, 1494, 1420, 1308, 1290, 1246, 1203, 1159, 882, 844, 767, 734, 645, 624, 610, 536, 495.

Procedure for the preparation of azobenzene-functionalized polyamide (3a, azoPA). 2,2-Bis[4-(4-aminophenyldiazenyl)phenoxy]phenyl]propane (2a; 0.6187 g, 1.000 mmol), N-methylpyrrolidinone (NMP, 10 mL) and pyridine (0.2 g) were added in a 50-mL, 3-necked flask equipped with a magnetic stirrer, nitrogen inlet and outlet, and stirred under dry nitrogen at room temperature for 30 min. After the solution was cooled to 0°C in an ice-water bath 4,4'-oxydibenzoyl chloride (1; 0.2940, 1.000mmol) was charged. The red solution was allowed to warm to room temperature overnight and poured into ethanol. The precipitate was collected, soxhlet extracted with ethanol and dried in vacuum oven to afford 0.84 g (100 %) of orange fibers. ATR-IR (cm^{-1}): 3312(H-bonded $\nu_{\text{N-H}}$), 3042, 2962, 1658 (amide I), 1591, 1524(amide II), 1489, 1403, 1304, 1230, 1169, 1149, 1098, 1013, 948, 872, 756, 543.

Procedure for the preparation of polyamide (PA, 3b). The control polyamide PA was prepared from 2,2-bis[4-(4-aminophenoxy)phenyl]propane (BPA, 0.4105, 1.000 mmol) and 4,4'-oxydibenzoyl chloride (1; 0.2940 g, 1.000 mmol) using the same procedure used for azoPA 3a to afford 0.62 (985) of white fibers. ATR-IR (cm^{-1}): 3306 (H-bonded $\nu_{\text{N-H}}$), 3038, 2964, 2811, 1648 (amide I), 1596, 1529 (amide II), 1492, 1404, 1306, 1217, 1166, 1099, 1081, 898, 827, 756, 558, 512.

Cast Films and Cantilevers. As described previously,⁴⁷ azoPI films were cast from the poly(amic acid) solution in

DMAc, involving vacuum evaporation of DMAc at 50 °C, and heat-treated at 100 °C/2 h, 150 °C/2 h, 175 °C/1 h, 200 °C/2 h, 250 °C/1 h, and 300 °C/1 h to form imidized polymers. The film thickness was approximately ca. 20 µm. The cantilever for this work was cut from the dried film with a pair of scissors. The cast films of azoPA and PA were prepared by first re-dissolving the dried polymer in DMAc, pouring the solution into a casting dish and using the same vacuum evaporation/heating protocol as that used in the preparation of azoPI film. The film thickness was approximately ca. 20 µm. Cantilevers with dimension of 6 mm (L) x 0.1 mm (W) x 0.02 mm (T) are cut from the cast films.

Instrumentation.

Proton nuclear magnetic resonance (NMR) spectra were measured at 300 MHz by a Bruker AVANCE 300 spectrometer. Differential scanning calorimetry (DSC) scans were conducted under nitrogen using a TA Instruments Q1000, using the standard heating rate of 10 °C/min Thermogravimetric analysis (TGA) was conducted in either nitrogen (N₂) or air atmosphere at a heating rate of 10°C/min using a TA Hi-Res TGA 2950 thermogravimetric analyzer. Wide angle X-ray diffraction (WAXD) experiments were carried out on a Statton box camera at 53 mm sample-to-image plate distances in transmission mode using Cu K α generated by a Rigaku Ultrax18 system. The mechanical properties of the materials in dynamic tension were investigated by a stress controlled dynamic mechanical analyzer (TA Instruments DMA Q800) at 1 Hz and 0.1% strain with a heating rate of 3°C/min in a nitrogen atmosphere. The glass transition temperatures were determined at the maximum tan δ (loss modulus/storage modulus). UV-vis absorption spectra of spin-cast films on quartz substrates were recorded on a Cary 5000 UV-vis-NIR spectrometer. Spin casting was conducted on a spin-coater by Specialty Coating Systems (Indianapolis, IN, USA), model SCS-6700. Polyamide or polyamic acid solution in DMAc (5wt%) was spread onto quartz substrates. Spin rate was set 500rpm for 30 sec, ramped up to 2000rpm in 10 sec and held for 60 sec. The films were then heat-treated using the schedule described in the film-casting procedure above. Fourier-transform infrared (FT-IR) spectra were measured by a Bruker Alpha-R spectrometer for routine characterization and by a Bruker FT-IR instrument (IFS 66v/s) in transmission mode for monitoring spectral changes during irradiation. The absorbance data were deconvoluted by using *OriginPro* software (ver. 9), and the data in Table 2 were obtained based on the area computation for each of deconvoluted peaks.

The irradiation of the film samples for (i) solid-state UV-vis experiment, (ii) real-time irradiation-DMA measurement under photostationary conditions, (iii) FTIR and (iv) photomechanical responses (bending angle) was conducted with a polarized, 445 nm LED light or a polarized, diode-pump solid state (DPSS, 445 nm) blue laser light. In each case, the polarization of the blue light was aligned parallel to long axis (x) of the cantilevers (E//x). The blue LED light intensity of 50 mW/cm² was used in experiments (i) and (ii); continuous-wave DPSS blue laser light at the intensity of 120 mW/cm² was used in experiments (iii)

and (iv). Photomechanical responses were characterized by monitoring the deflection of cantilevers with 6 x 1 x 0.02mm (width, length, and thickness). The magnitude of the photo-induced reduction in modulus (E') was examined in tension by placing the materials in a strain-controlled dynamic mechanical analyzer (DMA, TA Instruments RSA III). The films were held with a 4 x 10⁻⁵% strain to pre-stretch the film.

Acknowledgements

This work was completed at the Air Force Research Laboratory (AFRL) at Wright-Patterson Air Force Base with funding from Materials and Manufacturing Directorate as well as the Air Force Office of Scientific Research.

Conflicts of interest

There are no conflicts to declare.

Notes and references

- 1 R. Lovrien, *Proc. Natl. Acad. Sci. U. S. A.* **1967**, 57(2), 236-242.
- 2 J.-A. Lv, Y. Liu, J. Wei, E. Chen, L. Qin and Y. Yu, *Nature*, **2016**, 537, 179-184.
- 3 J. Gibson, X. Liu, S.V. Georgakopoulos, J.J. Wie, T.H. Ware and T.J. White, *IEEE Access* **2016**, 4, 2340-2348
- 4 G. Ugur, J. Chang, S. Xiang, L. Lin and J. Lu, *Adv. Mater.* **2012**, 24, 2685-2690.
- 5 J.J. Wie, D.H. Wang, V.P. Tondiglia, N.V. Tabiryan, R. O. Vergara-Tolosa, L.-S. Tan and T.J. White, *Macromol. Rapid Commun.* **2014**, 35, 2050-2056.
- 6 J. J. Wie, M. R. Shankar and T. J. White, *Nature Commun.* **2016**, 7, 13260.
- 7 A. H. Gelebart, D. J. Mulder, M. Varga, A. Konya, G. Vantomme, E. W. Meijer, R. L. B. Selinger and D. J. Broer, *Nature* **2017**, 546, 632-636.
- 8 X. Lu, S. Guo, X. Tong, H. Xia and Y. Zhao, *Adv. Mater.* **2017**, 29, 1606467/1-7. DOI: 10.1002/adma.20160646
- 9 (a) A. Fihey, A. Perrier, W. R. Browne, and D. Jacquemin, *Chem. Soc. Rev.* **2015**, 44, 3719-3759; (b) F. Ciardelli, M. Bertoldo, S. Bronco, A. Pucci, G. Ruggeri, and F. Signori, *Polym. Int.* **2013**, 62, 22-32. (c) M. Irie, *Bull. Chem. Soc. Jap.* **2008**, 81, 917-926.
- 10 S. K. Yesodha, C. K. Sadasivan Pillai and N. Tsutsumi, *Prog. Polym. Sci.* **2004**, 29, 45-74.
- 11 Cojocariu, C.; Rochon, P. *Pure Appl. Chem.* **2004**, 76, 1479-1497.
- 12 Viswanathan, N. K.; Kim, D. U.; Bian, S.; Williams, J.; Liu, W.; Li, L.; Samuelson, L.; Kumar, J.; Tripathy, S. K. *J. Mater. Chem.* **1999**, 9, 1941-1955.
- 13 Hugel, T.; Holland Nolan, B.; Cattani, A.; Moroder, L.; Seitz, M.; Gaub Hermann, E. *Science* **2002**, 296, 1103-1106.
- 14 (a) C. L. van Oosten, D. Corbett, D. Davies, M. Warner, C. W. M. Bastiaansen and D. J. Broer, *Macromolecules* **2008**, 41, 8592-8596; (b) D. Corbett, M. Warner, *Liquid Crystals* **2009**, 36, 1263-1280; (c) D. Corbett, M. Warner, *Phys. Rev. E: Stat. Nonlinear, Soft Mat. Phys.* **2008**, 77, 051710/1; (d) D. Corbett, M. Warner, *Phys. Rev. Lett.* **2007**, 99, 174302/1.
- 15 Natansohn, A.; Rochon, P. *Chem. Rev.* **2002**, 102, 4139-4175.
- 16 Lee, K. M.; Koerner, H.; Vaia, R. A.; Bunning, T. J.; White, T. J. *Soft Matter* **2011**, 7, 4318-4324.

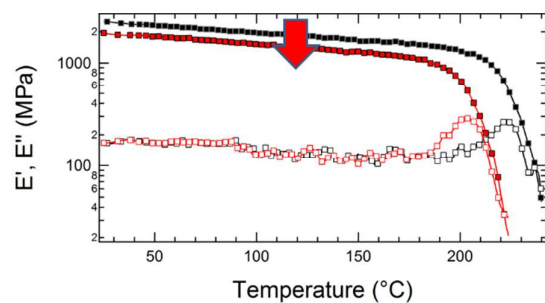
- 17 Wang, D. H.; Lee, K. M.; Yu, Z.; Koerner, H.; Vaia, R. A.; White, T. J.; Tan, L. S. *Macromolecules* **2011**, *44*, 3840-3846.
- 18 Lee, K. M.; Wang, D. H.; H Koerner; RA Vaia; LS Tan; White, T. J. *Angew. Chem. Int. Ed.*, **2012**, *124*, 4193-4197.
- 19 Lee, K. M.; Koerner, H.; Vaia, R. A.; Bunning, T. J.; White, T. J. *Macromolecules* **2010**, *43*, 8185-8190.
- 20 Lee, K. M.; Smith, M. L.; Koerner, H.; Tabiryan, N. V.; Vaia, R. A.; Bunning, T. J.; White, T. J. *Adv. Funct. Mater.* **2011**, *21*, 2913-2918.
- 21 White, T. J.; Tabiryan, N.; Tondiglia, V. P.; Serak, S.; Hrozhyk, U.; Vaia, R. A.; Bunning, T. J. *Soft Matter* **2008**, *4*, 1796-1798.
- 22 (a) Hrozhyk, U.; Serak, S.; Tabiryan, N.; White, T. J.; Bunning, T. J. *Opt. Express* **2009**, *17*, 716-722. (b) Tabiryan, N.; Serak, S.; Dai, X.-M.; Bunning, T. J. *Opt. Express* **2005**, *13*, 7442-7448.
- 23 White, T. J.; Serak, S. V.; Tabiryan, N. V.; Vaia, R. A.; Bunning, T. J. *J Mater. Chem.* **2009**, *19*, 1080-1085.
- 24 Serak, S.; Tabiryan, N. Y.; White, T. J.; Vaia, R. A.; Bunning, T. J. *Soft Matter* **2010**, *6*, 779-783.
- 25 Lee, K. M.; Tabiryan, N. V.; Bunning, T. J.; White, T. J. *J. Mater. Chem.* **2012**, *22*, 691-698.
- 26 L. T. de Haan, C. Sánchez-Somolinos, C. M. W. Bastiaansen, A. P. H. J. Schenning and D. J. Broer, *Angew. Chem., Int. Ed.* **2012**, *51*, 12469-12472.
- 27 K. M. Lee, T. J. Bunning and T. J. White, *Adv. Mater.* **2012**, *24*, 2839-2843.
- 28 M. E. McConney, A. Martinez, V. P. Tondiglia, K. M. Lee, D. Langley, I. I. Smalyukh and T. J. White, *Adv. Mater.* **2013**, *25*, 5880-5885.
- 29 J. J. Wie, K. M. Lee, M.L. Smith, R.A. Vaia and T.J. White, *Soft Matter* **2013**, *9*, 9303-9310.
- 30 D. H. Wang, K. M. Lee, Z. N. Yu, H. Koerner, R. A. Vaia, T. J. White and L.-S. Tan, *Macromolecules* **2011**, *44*, 3840-3846.
- 31 K. M. Lee, D. H. Wang, H. Koerner, R. A. Vaia, L.-S. Tan and T. J. White, *Angew. Chem., Int. Ed.* **2012**, *51*, 4117-4121.
- 32 D. Roberts, M. Worden, S. Chowdhury and W.S. Oates, *Modelling Simul. Mater. Sci. Eng.* **2017**, *25*, 055009 (28pp).
- 33 W. T. Astbury, *Trans. Faraday Soc.* **1933**, *29*, 193-211.
- 34 M. C. Huggins, *J. Chem. Phys.* **1940**, *8*, 598-600.
- 35 C. M. Paleos, D. Tsiourvas, *Adv. Mater.* **1997**, *9*, 695-710.
- 36 N. Khazanovich, J. R. Granja, D. E. McRee, R. A. Milligan and M. R. Ghadiri, *J. Am. Chem. Soc.* **1994**, *116*, 6011-6012.
- 37 W. H. Binder, R. Zirbs, in W. H. Binder, ed. *Hydrogen Bonded Polymers*, *Adv. Polym. Sci.* Springer-Verlag, Berlin, **2007**, *207*, 1-78.
- 38 L. Brunsveld, B. J. B. Folmer, E. W. Meijer and R. P. Sijbesma, *Chem. Rev.*, **2001**, *101*, 4071-4097.
- 39 H. Zhang, L. Ye and K. Mosbach, *J. Mol. Recognit.* **2006**, *19*, 248-259.
- 40 S. Chen, W. H. Binder, *Acc. Chem. Res.* **2016**, *49*, 1409-1420.
- 41 M. Afshari, D. J. Sikkema, K. Lee, and M. Bogle, *Polymer Reviews* **2008**, *48*, 230-274.
- 42 A. A. Leal, J. M. Deitzel, S. H. McKnight, J. W. Gillespie, *Polymer* **2009**, *50*, 2900-2905.
- 43 A. Kozanecka-Szmigiela, J. Konieczkowskab, K. Switkowskia, J. Antonowicza, B. Trzebickab, D. Szmigielc, E. Schab-Balcerzak, *J. Photochem. Photobiol.-A Chem.* **2016**, *318*, 114-123.
- 44 K. M. Lee, H. Koerner, D. H. Wang, L.-S. Tan, T. J. White and R. A. Vaia, *Macromolecules* **2012**, *45*, 7527-7534.
- 45 K. M. Lee, D. H. Wang, H. Koerner, R. A. Vaia, L.-S. Tan and T. J. White, *Macromol. Chem. Phys.* **2013**, *214*, 1189-1194.
- 46 D. H. Wang, J. J. Wie, K. M. Lee, T. J. White and L.-S. Tan, *Macromolecules* **2014**, *47*, 659-667.
- 47 J. J. Wie, D. H. Wang, K. M. Lee, L.-S. Tan and T. J. White, *Chem. Mater.* **2014**, *26*, 5223-5230.
- 48 J. J. Wie, S. Chatterjee, D. H. Wang, L.-S. Tan, M. R. Shankar and T. J. White, *Polymer* **2014**, *55*, 5915-5923.
- 49 K. M. Lee, D. H. Wang, H. Koerner, R. A. Vaia, L.-S. Tan and T. J. White, *Macromol. Chem. Phys.* **2013**, *214*, 1189-1194.
- 50 H. S. Blair, H. I. Pague and J. E. Riordan, *Polymer* **1980**, *21*, 1195-1198. This paper reported the first example of azoPA film that exhibited photomechanical effect at room temperature. However, this azoPA is derived from a monomer containing two secondary amines (2,5-dimethylpiperazine), and azodibenzoic acid chloride and does not have any hydrogen bonds in the material.
- 51 The empirical formula and formula weight for each repeat unit (RU) of PA and azoPA are: C₅₅H₃₆N₆O₇; FW = 892.91 and C₅₃H₄₀N₆O₅ FW=840.92, respectively. Given the same degree of polymerization, the molecular weight of azoPA RU is ~ 6% greater than azoPA RU.
- 52 M. L. Baczowski, D. H. Wang, D. H. Lee, K. M. Lee, M. L. Smith, T. J. White and L.-S. Tan, *ACS Macro Letters* **2017**, *6*, 1432-1437.
- 53 (a) H-bonded cis-conformer of benzanilide dimer was proposed by G. Q. Tang, J. MacInnis, M. Kasha, *J. Am. Chem. Soc.* **1987**, *109*, 2531-2533. (b) E. J. O'Connell, Jr, M. Delmauro and J. Irwin, *Photochem. Photobiol.* **1971**, *14*, 189-95. (c) J. Heldt, J. R. Heldt and E. Szatan, *J. Photochem. Photobiol. A Chem.* **1999**, *121*, 91-97, and references therein.
- 54 (a) Steiner, T. *Angew. Chem. Inter. Ed.* **2002**, *41*, 48-76. (b) G. A. Jeffrey, *An Introduction to Hydrogen Bonding*, Oxford, University Press, Oxford, 1997.
- 55 M. Petr, M.E. Helgeson, J. Soulages, G.H. McKinley and P.T. Hammond, *Polymer* **2013**, *54*, 2850-2856.
- 56 J. Vapaavuori, Z. Mahimwalla, R.R. Chromik, M. Kaivola, A. Priimagi and C.J. Barrett, *J. Mater. Chem. C* **2013**, *1*, 2806-2810.
- 57 P. Karageorgiev, D. Neher, B. Schulz, B. Stiller, U. Pietsch, M. Giersig and L. Brehmer, *Nature Materials* **2005**, *4*, 699-.
- 58 M. Saphiannikova and V. Toshchevikov, *J. Soc. Inform. Display* **2015**, *23*, 146-153.
- 59 (a) A. F. Yee and S. A. Smith, *Macromolecules* **1981**, *14*, 54-64; (b) P. Tekely and E. Turska, *Polymer* **1983**, *24*, 667-672.
- 60 For the representative assignment of amide I and II bands for aromatic polyamides, see Tamami, B.; Yeganeh, H. *Polymer* **2001**, *42*, 415-420.
- 61 N. B. Colthup, L. H. Daly and S. E. Wiberley, *Introduction to Infrared and Raman Spectroscopy*, 3rd Ed, Academic Press, 1990, San Diego, CA USA, pg.351.
- 62 S. Krimm and J. Bandekar, *Adv. Protein Chem.*, **1986**, *38*, 181-364.
- 63 S. Trifan and J. F. Terenzi, *J. Polym. Sci.* **1958**, *28*, 443-445.
- 64 M. C. Tobin and M. J. Carrano, *J. Chem. Phys.* **1956**, *25*, 1044-1052.
- 65 L. R. Schroeder and S. L. Cooper, *J. Appl. Phys.* **1976**, *47*, 4310-4317.



ARTICLE

Graphical Abstract

Azo-Polyamide (azoPA)

**azoPA: Dissociation of inter-chain H-bonding**

Azo-Polyimides (azoPI)

**azoPI: Enhanced intra-chain segmental mobility**